Cellular Physiology and Biochemistry

Cell Physiol Biochem 2017;42:999-1012
DOI: 10.1159/000478682
Published online: June 27, 2017
Accepted: May 16, 2017

Original Paper

LncRNA SNHG6 is Associated with Poor Prognosis of Gastric Cancer and Promotes Cell Proliferation and EMT through Epigenetically Silencing p27 and Sponging miR-101-3p

Kai Yan[a] Jie Tian[b] Wenzheng Shi[c] Hao Xia[a] Yuanfang Zhu[a]

[a]Department of Gastrointestinal Surgery, Clinical Medical College of Yangzhou University (Northern Jiangsu People's Hospital), Yangzhou, [b]Department of Pathology, Clinical Medical College of Yangzhou University (Northern Jiangsu People's Hospital), Yangzhou, [c]Department of General Surgery, The First Hospital of Tsinghua University, Beijing, China

Key Words
Gastric cancer • SNHG6 • EZH2 • p27 • miR-101-3p • ZEB1 • EMT

Abstract
Background/Amis: Long non-coding RNAs (lncRNAs), a novel class of transcripts, have been shown to play critical roles in diverse cellular biological processes, including tumorigenesis. Small nucleolar RNA host gene 6 (SNHG6) regulates various biological processes in cancer cells. However, the biological role of SNHG6 in gastric cancer still remains to be explored. The aim of this study is to investigate the characteristic of the SNHG6 in gastric cancer. ***Methods:*** Quantitative real-time polymerase chain reaction (qRT-PCR) was used to measure the expression of SNHG6 in gastric cancer tissues and cell lines. MTT assays, colony formation assays were used to determine the impact of SNHG6 on tumorigenesis . Flow cytometric analysis of cell cycle and apoptosis was performed to measure the effect of SNHG6 on cell cycle and apoptosis rate. Transwell assay was performed to measure the effect of SNHG6 on cell migration. Western blotting and immunofluorescence were utilized to examine the effect of SNHG6 on epithelial–mesenchymal transition (EMT) of GC cells. Chromatin immunoprecipitation (ChIP), RNA immunoprecipitation (RIP), RNA-pulldown and luciferase reporter assays were employed to dissect molecular mechanisms. ***Results:*** In this study, we revealed that SNHG6 was overexpressed in gastric cancer tissues and cell lines. High expression levels of SNHG6 wereassociated with invasion depth, lymph node metastasis, distant metastasis and tumor/node/metastasis (TNM) stage, and predicted poor prognosis. Loss-of-function assays revealed that silenced SNHG6 obviously inhibited gastric cancer cell growth, weakened cell migration capacity and suppressed the EMT processes of gastric cancer cells. Additionally, ChIP, RIP, RNA-pulldown and luciferase reporter assays evidenced that SNHG6 could epigenetically silenced p27 and could competitively sponging miR-101-3p thereby regulating zinc finger E-box-binding homeobox 1 (ZEB1). ***Conclusion:*** In summary,

Jie Tian

Department of Pathology, Clinical Medical College of Yangzhou University (Northern Jiangsu People's Hospital), No. 98, West Nantong Rd, Yangzhou 225001, China)
E-Mail gastroenterology@qq.com

our findings demonstrated that SNHG6 acted as an oncogene in gastric cancer cells through regulating miR-101-3p/ZEB1 at a post-transcriptional level and silencing expression at a transcriptional level by recruiting enhancer of zeste homolog 2 (EZH2) to the promoter of p27. SNHG6 might serve as a candidate prognostic biomarker and a target for novel therapies of gastric cancer patients.

Introduction

Gastric cancer (GC) is one of the most common malignancies and the second leading cancer-related deaths worldwide [1, 2]. Despite many efforts have been made in diagnostic techniques and therapeutic measures, the clinical outcome of GC patients still remain unsatisfied [3, 4]. Since gastric carcinogenesis is a complicated biological process involving multiple oncogenes or tumor suppressors' dysregulation [5-10], investigating the molecular mechanisms is essential for exploring sensitive or effective biomarkers for early diagnosis and novel treatment for improving GC patients' survival rate.

Currently, with development of sequencing technologies and the deepening of researches, many long non coding RNAs (lncRNAs), a class of transcripts longer than 200nt with little or no protein-coding potential, are uncovered and investigated. Because of involving in multiple cellular biological processes especially in tumorigenesis [11-13], lncRNAs have been attracting many researchers attention. For instance, lncRNA Unigene56159 promotes epithelial-mesenchymal transition of hepatocellular carcinoma cells at a post-transcriptional level through sponging miR-140-5p [14]. Zhou et al. reported that the interaction between miR-141 and lncRNA-H19 in regulating cell proliferation and migration in gastric cancer [15]. In addition to post-transcriptional level, TUG1 was involved in the transcriptional repression of the CELF1 and regulated non-small cell lung cancer progression by binding to polycomb repressive complex 2 (PRC2) [16]. Recently, plenty lncRNAs have been reported to play critical role in tumorigenesis through recruiting PRC2. PRC2, a methyltransferase composed with enhancer of zeste homolog 2 (EZH2), suppressor of zeste 12 (SUZ12) and embryonic ectoderm development (EED), can modulate gene expression through catalyzing the di- and trimethylation of lysineresidue 27 of histone 3 (H3K27me3). The interaction between PRC and lncRNAs has been reported in multiple cancers [17-19].

Currently, some snoRNAs exhibit differential expression patterns in various human cancers and demonstrate the ability to affect cell transformation, tumorigenesis, and metastasis. snoRNA host gene 6 (SNHG6) have been demonstrated to be as a potential oncogene involved in the initial and development of hepatocellular carcinoma [20, 21]. However, activities of SNHG6 in GC tumorigenesis have not been well characterized, which prompted us to explore the role of SNHG6 in human GC. In our study, we revealed that SNHG6 was significantly increased in GC tissues, cell lines and was associated with poor prognosis of GC patients. Additionally, silenced SNHG6 inhibited GC cell proliferation, migration and reversed EMT to MET. Mechanism experiments uncovered that si-SNHG6 mediated growth inhibition was attributed to its influence on cell cycle through interacting with PRC2 and epigenetic silencing p27, while si-SNHG6 mediated migration-inhibition was through sponging miR-101-3p and thus regulating the expression of ZEB1. Our study may provide a strategy and facilitate the development of lncRNA-directed diagnostics and therapeutics against GC.

Materials and Methods

Clinical specimens

GC specimens and the corresponding adjacent tissues were collected from patients with GC at Department of Gastrointestinal Surgery, Clinical Medical College of Yangzhou University (Northern Jiangsu People's Hospital) between 2010 and 2013. All the informed consent was obtained. The diagnosis of GC

Table 1. The list of primers

Gene	Forward primer	Reverse primer
Human qRT-PCR		
SNHG6	CCTACTGACAACATCGACGTTGAAG	GGAGAAAACGCTTAGCCATACAG
P15	TCTCCGTTGGCCGGAGGTCA	TGCGCAGGTACCCTGCAACG
P16	CCAGCGCATCGCGTCTC	TAGAGATCGCCGCTTGGA
P21	GGCTGTCTCCGCTCATAG	CAGCAGACCACCATTTCA
P27	GGTGTCTAGGTGCTCCAGGT	GCACTCTCCAGGAGGACACA
P57	GGTGTCTAGGTGCTCCAGGT	GCACTCTCCAGGAGGACACA
ZEB1	TAAAGTGGCGGTAGATGGTA	ACTGTTTGTAGCGACTGGATT
GAPDH	GGGAGCCAAAAGGGTCAT	GAGTCCTTCCACGATACCAA
ChIP primer		
P27	AAGTGCCGCGTCTACTCCTG	TGGAGGCAGTGGGCAATGGT

was histopathologically confirmed and no local or systemic treatment was conducted before surgery. The protocols used in the study were approved by the Hospital's Protection of Human Subjects Committee.

Cell culture and transfection

GC cell lines (MGC-803, AGS, SGC-7901, BGC-823), in comparison to normal gastric epithelial cell line (GES-1) were purchased from the Cell Bank of Type Culture Collection (CBTCC, Chinese Academy of Sciences, Shanghai, China). MGC-803 and BGC-823 cells were cultured in RPMI 1640 (Invitrogen); GES, SGC-7901 and AGS cells were cultured in DMEM supplemented with 10% fetal bovine serum (Gibco, Carlsbad, CA, USA). The cells were washed with 1*phosphate buffer saline (PBS) (pH7.4) and then transiently transfected with 50 nmol/l si-NC, si-SNHG6 or si-p27 using Lipofectamine 2000 (Invitrogen) following the manufacturer's instructions.

RNA extraction and qRT-PCR assays

Total RNA from specimens and cells was isolated with TRIzol reagent (Invitrogen, Karlsruhe, Germany) based on the manufacturer's instructions. Quantitative real-time polymerase chain reaction (qRT-PCR) was performed using the PrimeScript RT Reagent Kit and SYBR Premix Ex Taq (TaKaRa, Dalian, China) following the manufacturer's instructions. The results were normalized to the expression of glyceraldehyde-3-phosphate dehydrogenase (GAPDH). The specific primers used are presented in Table 1. PCR results were analyzed to obtain Ct values of amplified products, and data was analyzed by adopting $2^{-\Delta\Delta Ct}$ method.

Cell viability

Cell viability was assessed via 3-(4,5-dimethylthiazol-2-yl)-2, 5-diphenyl-trtrazolium bromide (MTT) assay. 5×10^3 cells/well transfected with indicated vector were seeded in a 96-well flat-bottomed plate for 24 h and cultured in normal medium. At 0, 24, 48, 72 h and 96h after transfection, the MTT solution (5 mg/ml, 20 µl) was added to each well. Following incubation for 4 h, the media was removed and 100 µl DMSO were added to each well. The relative number of surviving cells was assessed by measuring the optical density (O.D.) of cell lysates at 560 nm. All assays were performed in triplicate.

Colony formation assay

Cells (500 cells/ well) transfected with indicated vector were plated in 6-well plates and incubated at 37 °C. Two weeks later, the cells were fixed and stained with 0.1% crystal violet. The number of visible colonies was counted manually.

Cell migration assay

Cell migration were measured by transwell chamber (8 um pore size, Corning). 48 h after transfection, cells in serum-free media were placed into the upper chamber. Media containing 10% FBS was added into the lower chamber. Following 48 h incubation, cells remaining in upper membrane were wiped off, while cells that migrated were fixed in methanol, stained with 0.1% crystal violet and counted under a microscope. Three independent experiments were carried out. Cells adhering to the bottom surface of the membrane were counted in five randomly selected areas under microscope field. Each experiment was repeated three times.

Flow cytometric analysis of apoptosis

Cells transfected with indicated plasmid or negative control were reaped after 48 hours. Apoptosis were performed using flow cytometric analyses with Annexin V: FITC Apoptosis Detection Kits (BD Biosciences, USA), according to the manufacturer's instructions. All samples were assayed in triplicate.

Flow cytometric analysis of cell cycle distribution

Cells were collected directly or 48 hours after transfection and washed with ice-cold phosphate-buffered saline (PBS), and fixed with 70% ethanol overnight at -20°C. Fixed cells were rehydrated in PBS for 10 minutes and incubated in RNase A (1mg/ml) for 30 min at 37°C, then the cells were subjected to PI/RNase staining followed by flow cytometric analysis using a FACScan instrument (Becton Dickinson, Mountain View, CA). All samples were assayed in triplicate.

Immunofluorescence

Cells seeded on glass coverslips in 6-well plates were fixed in 4% formaldehyde solution and permeabilized with 0.5% Triton X-100/PBS. Cells were blocked with 5% BSA-PBS for 1h at room temperature and incubated with primary antibody at 4°C overnight, followed by incubation with fluorescent-dye conjugated secondary antibody (Invitrogen) for 1h, and then stained with DAPI. Finally, images were taken under an inverted fluorescence microscope.

Luciferase assay

Luciferase activity was measured using a Dual Luciferase Assay Kit (Promega, Madison, WI, USA) according to the manufacturer's instructions.

Western blot analysis

Total protein was extracted from cells and tumor tissues using RIPA lysis buffer. Extracted proteins were mixed with loading buffer, subject to 10% SDS-PAGE and transferred to PVDF membranes, which were subsequently blocked in a 5% solution of non-fat milk for 2 h. The membranes were subsequently incubated with antibodies specific to E-cadherin, N-cadherin, Vimentin, β-catenin and ZEB1 (Abcam, Cambridge, UK) for 16 h. GAPDH expression was used as an internal reference.

Subcellular fractionation location

The separation of nuclear and cytosolic fractions was performed using the PARIS Kit (Life Technologies) according to the manufacturer's instructions. In detail, Collect up to 10^7 fresh cultured GC cells, wash once in PBS, and place washed cells on ice; resuspend cells in 100–500 μL ice-cold cell fractionation buffer; incubate on ice 5–10 min; centrifuge samples 1–5 min at 4°C and 500 xg; carefully aspirate the cytoplasmic fraction away from the nuclear pellet and wash the nuclear pellet in ice-cold cell fractionation buffer; then lyse nuclear pellet in cell disruption buffer and split the sample for RNA isolation. For RNA isolation, mix the lysate with an equal volume of 2X Lysis/Binding Solution; add 1 "sample volume" of 100% ethanol to the mixture; wash with wash solution; elute RNA with elute solution. RNAs extracted from each of the fractions were subjected to following RT–qPCR analysis to demonstrate the levels of nuclear control transcript (U6), cytoplasmic control transcript (GAPDH), SNHG6. PCR primers were provided in Table 3.

Chromatin immunoprecipitation (ChIP)

We performed chromatin immunoprecipitation (ChIP) using the EZ ChIP™Chromatin Immunoprecipitation Kit for cell line samples (Millipore, Bedford, MA). Briefly, we sonicated the crosslinked chromatin DNA into 200-to 500-bp fragments. Normal mouse IgG was used as the negative control. The primer sequences are listed in Table 3. The antibodies for the ChIP assays were obtained from Millipore. Quantification of the immunoprecipitated DNA was performed using qPCR with SYBR Green Mix (Takara). The ChIP data were calculated as a percentage relative to the input DNA using the equation 2[Input Ct-Target Ct] × 0.1 × 100.

RNA immunoprecipitation(RIP)

We performed RNA immunoprecipitation (RIP) experiments using the Magna RIP™RNA-Binding Protein Immunoprecipitation Kit (Millipore, USA) according to the manufacturer's instructions. The

antibodies for the RIP assays of Ago2, EZH2, EED, SUZ12 were obtained from Abcam. The total RNAs were the input controls.

RNA pulldown assay

Biotin-labeled RNAs were transcribed *in vitro* with the Biotin RNA Labeling Mix (Roche Diagnostics) and T7 RNA polymerase (Roche Diagnostics), treated with RNase-free DNase I (Roche), and purified with an RNeasy Mini Kit (Qiagen, Valencia, CA). Next, 1 mg whole-cell lysates from BGC-823 cells was incubated with 3 μg of purified biotinylated transcripts for 1 h at 25 °C. Complexes were isolated with streptavidin agarose beads (Invitrogen). The beads were washed briefly three times and boiled in sodium dodecyl sulfate (SDS) buffer, and the retrieved protein was detected using the standard western blot technique.

Statistical analysis

The SPSS 17.0 statistical analysis software was used for the statistical analysis of the experimental data. The significance of differences between groups was estimated by Student's t-test. Multiple group comparisons were analyzed with one-way ANOVA. Statistically significant correlation between SNHG6 and ZEB1 or p27 expression levels in GC tissues was analyzed by Spearman's correlation analysis. The overall survival probability was analyzed using Kaplan-Meier methods and evaluated using the log-rank test. Cox proportional hazards regression model was generated to identify factors associated with overall survival through a multivariate survival analysis of GC. A P value less than 0.05 were considered significant.

Results

SNHG6 is upregulated in human GC tissues and cell lines

To explore the function of SNHG6 in GC, we first performed qRT-PCR to measure the level of SNHG6 in 78 GC tissues and cell lines. Comparing with matched adjacent normal tissues, SNHG6 level was significantly increased in GC tissues (Fig. 1A, $p<0.01$). High level of SNHG6 was also confirmed in four GC cell lines (MGC-803, AGS, SGC-7901, BGC-823), in comparison to normal gastric epithelial cell line (GES-1) (Fig. 1B, $p<0.01$). Furthermore, we evaluated the correlation of SNHG6 and clinical pathological features. The median value of SNHG6 in all GC tissues was used as a cutoff value, and all samples were divided into two group (high expression group n=45 vs. low expression group n =33). As shown in Table 2, increased level of SNHG6 was significantly correlated with tumor invasion depth (p=0.001), lymph node metastasis (p=0.012), distant metastasis (p=0.006) and TNM stage (p=0.001), but was no significant correlation with sex, age and histological grade ($p>0.05$). Additionally,

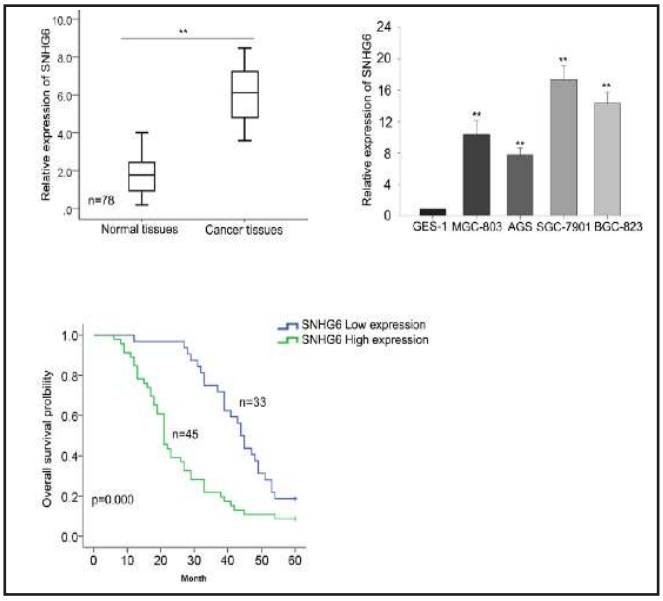

Fig. 1. SNHG6 is upregulated in human GC tissues and cell lines. A. Relative expression of SNHG6 in GC tissues (n=78) compared with the corresponding normal tissues (n=78). SNHG6 expression was examined by quantitative real-time PCR (qRT-PCR) and normalized to GAPDH expression. B. The expression level of SNHG6 in four GC cell lines and normal GES-1 cells. Assays were performed in triplicate. C. Kaplan-Meier survival analysis revealed that high-level of SNHG6 was associated with poor prognosis in patients with GC. *P<0.05, **P<0.01, Means±SD, was shown.

Kaplan–Meier method analysis (log-rank test) determined that patients with high level of SNHG6 had a significantly shorter overall survival than those with low level of SNHG6 (Fig. 1C, P=0.000). Proportional hazards method analysis revealed that high level of SNHG6 could be acted as prognostic factor (Table 3, P =0.009). These data together indicated that SNHG6 might be involved in the progression of GC.

Silenced SNHG6 suppresses cell proliferation through causing G1 arrest and inducing apoptosis in GC cells

To determine the biological function of SNHG6 in GC cells, we selected SGC-7901 and BGC-823 cells which express relative high level of SNHG6 and transfected two cell lines with SNHG6 specific siRNA (Fig. 2A). To assess the effect of SNHG6 on GC cell proliferation ability, we performed MTT and colony formation. As shown in Fig. 2B, results from MTT assays present that cells silenced SNHG6 displayed a weakened viability. Similarly, colony formation assays revealed that colony-formation efficiency was significantly suppressed when SNHG6 was knockdown (Fig. 2C). To determine SNHG6 pro-proliferation mechanism, flow cytometric analysis of cell cycle distribution and apoptosis rate were utilized. As obtained in Fig. 2D-E, silenced SNHG6 caused G0/G1 arrest and significantly increased the apoptosis rate. These investigations proved the oncogene effect of SNHG6 on GC cells and such function was attributed to its influence on cell cycle and apoptosis.

SNHG6 knockdown represses cell migration and reverses EMT to MET

To examine the effect of SNHG6 on cell migration capacity, transwell assays were performed and the results revealed that deletion of SNHG6 decreased BGC-823 and SGC-7901 cell migration capacity (Fig. 3A). As EMT is a critical process contributing to tumor metastasis, we assessed the function of SNHG6 on EMT markers. As observed in Fig. 3B, western blot showed that inhibition of SNHG6 decreased the mesenchymal markers (N-cadherin, vimentin) whereas increased epithelial markers (E-cadherin, β-catenin); and the level of ZEB1, a crucial transcription factor that regulates EMT was

Table 2. Correlation between SNHG6 Expression and Clinical Features. (n=78)

Variable	LncRNA-SNHG6 Expression		P-value
	low	high	
Gender			
Male	15	17	0.484
Female	18	28	
Age			
≤60	14	23	0.649
>60	19	22	
Histological grade			
Low or undiffer	20	24	0.487
Middle or high	13	21	
Tumor invasion depth			
T1	22	13	0.001*
≥T2	11	32	
Lymph node metastasis			
N0	14	24	0.012*
≥N1	19	21	
Distant metastasis			
M0	21	13	0.006*
M1	12	32	
TNM stage			
I-II	20	12	0.001*
III-IV	13	33	

Table 3. Multivariate analysis of prognostic parameters in patients with gastric cancer by Cox regression analysis. Proportional hazards method analysis showed a positive, independent prognostic importance of SHNG6 expression (P = 0.009), in addition to the independent prognostic impact of Lymph node metastasis (P = 0.000) and TNM stage (P=0.011). *P < 0.05 was considered statistically significant

Variable	Category	P-value
Gender	Male	0.898
	Femal	
Age	≤60	0.130
	>60	
Histological grade	Low or undiffer	0.265
	Middle or high	
Tumor invasion depth	T1	0.389
	≥T2	
Lymph node metastasis	N0	0.000*
	≥N1	
Distant metastasis	M0	0.289
	M1	
TNM stage	I-II	0.011*
	III-IV	
SNHG6 expression	Low	0.009*
	High	

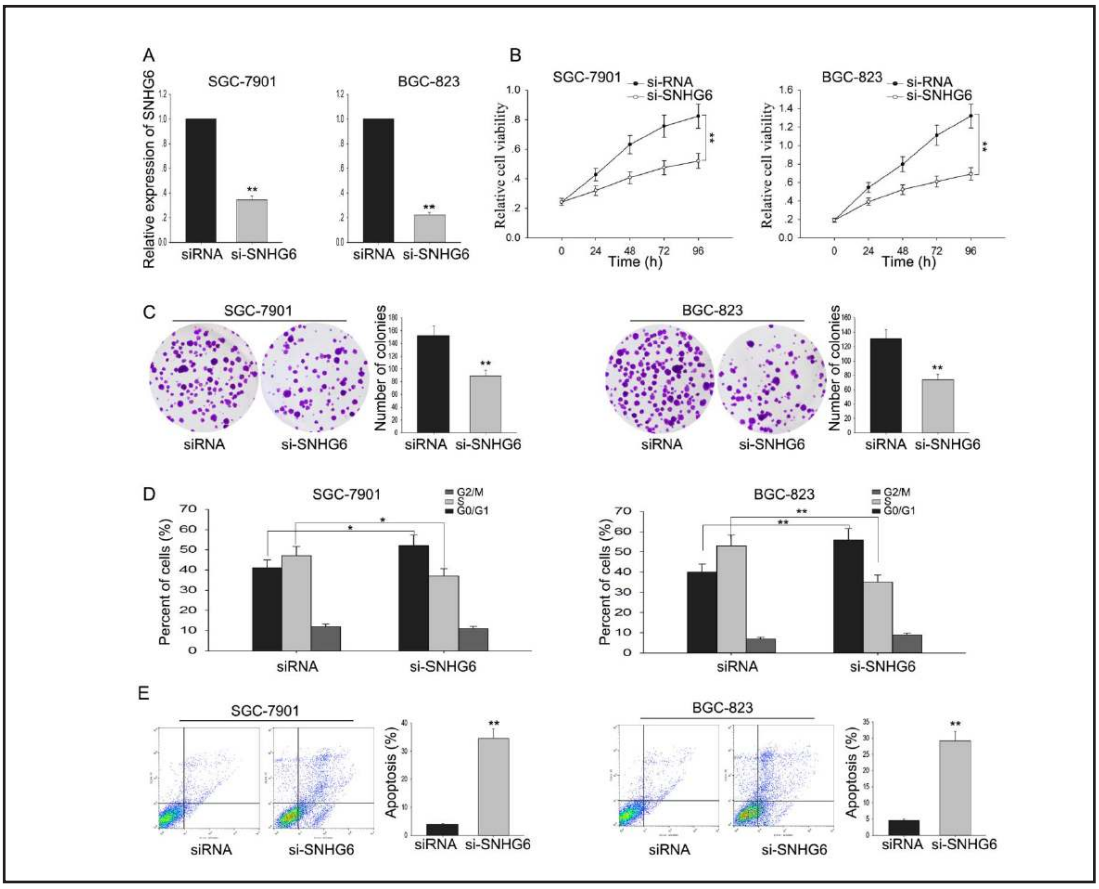

Fig. 2. Silenced SNHG6 suppresses cell proliferation through causing G1 arrest and inducing apoptosis in GC cells. A. The results of qPCR determined that the relative expression of SNHG6 decreased by transfection with si-SNHG6 in GC cells, compared with the transfection with si-NC. B-C. MTT and colony formation assays were performed to measure the proliferation ability of GC cells transfected with si-SNHG6 compared with the cells transfected with si-NC. D-E. Flow cytometric analysis was used to determine the effect of SNHG6 knockdown on cell cycle and apoptosis. *P<0.05, **P<0.01, Means±SD, was shown.

also reduced significantly. Consistent with western blot, results from immunofluorescence further verified the effect of SNHG6 on EMT formation (Fig. 3C). These findings revealed that SNHG6 potentially influenced the migration capacity and EMT phenotype formation of GC cells and such function might be exerted by regulating ZEB1 expression

SNHG6 exerted its function through epigenetically silencing p27 transcription and sponging miR-101-3p

To investigate the underlying mechanism of SNHG6 in GC cells, we measured the percentage of SNHG6 in the cytoplasmic and nuclear fractions of BGC-823 and SGC-7901 cells. As observed in Fig. 4A, SNHG6 located both in cytoplasma and nucleus. Since accumulating documents have revealed that lncRNAs could interacted with PRC2 and SNHG6 has been identified as competing endogenous (ce)RNAs regulating ZEB1 through sponging miRNA-101-3p [21], we speculated that the potential mechanism of SNHG6 in GC cells might involve both transcriptional and post-transcriptional regulation. To test this prediction, we first confirmed the regulatory pathway between SNHG6 and miR-101-3p. As revealed in Fig. 4B-D, results from RIP, luciferase reporter assay and biotin-avidin pulldown assay indicated that SNHG6 regulated miR-101-3p in a ceRNA manner. ZEB1, a key regulator of EMT, is identified as a target of miR-101-3p by luciferase reporter assay and western blot assay (Fig. 4E-F).

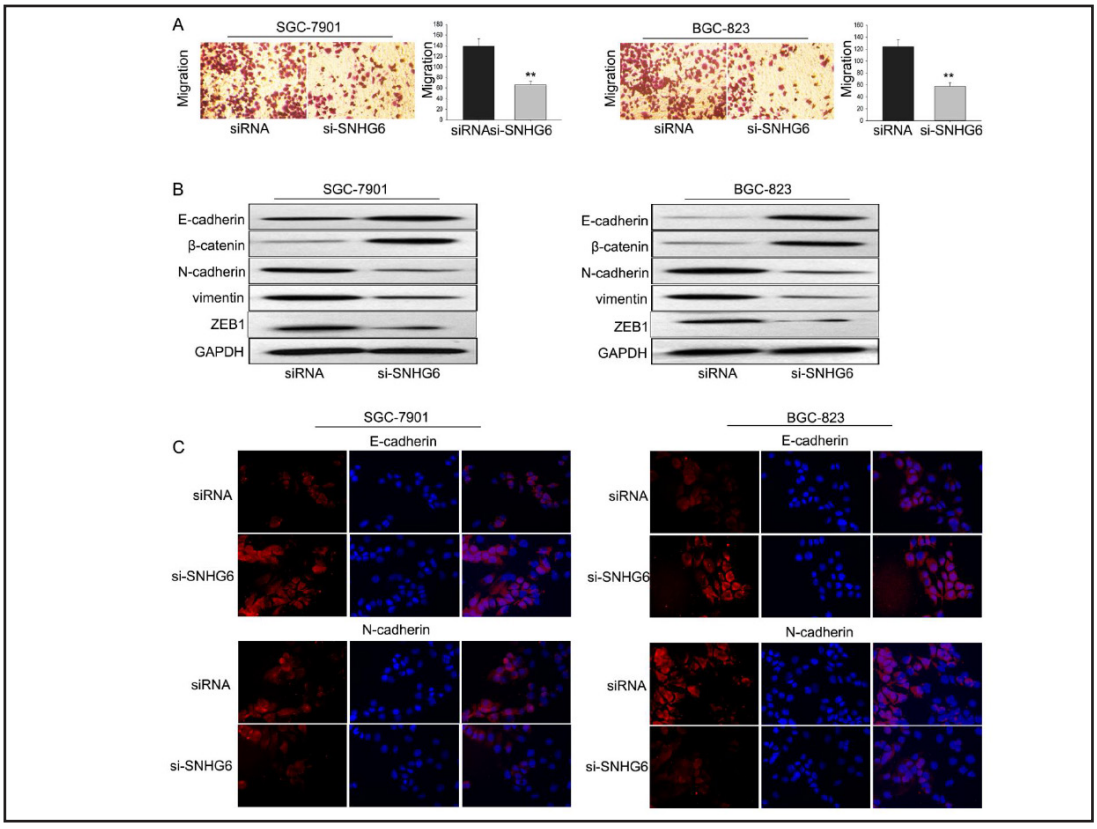

Fig. 3. Knockdown SNHG6 represses cell migration and reverses EMT to MET. A. Transwell assay was applied to measure the effect of SNHG6 deletion on cell migration capacity. B. Western blot assay was utilized to detect the influence of SNHG6 silenced on cell epithelial makers (E-cadherin, β-catenin), mesenchymal makers (N-cadherin, Vimentin) and the level of ZEB1. C. Expression of EMT makers in GC cells after SNHG6 knockdown was analyzed by immunofluorescence. *P<0.05, **P<0.01, Means±SD, was shown.

Therefore, the pro-metastasis function of SNHG6 was through regulating ZEB1 via acting as a ceRNA competitively sponging miR-101-3p.

Next, we investigated the pro-proliferation mechanism of SNHG6. Due to the effect of SNHG6 on cell cycle, we measured the level CKIs (p15, p16, p17, p21, p27, p57). As shown in Fig. 5A, the p27 was significantly increased when SNHG6 was deleted. Since SNHG6 also located in nucleus, we speculated that SNHG6 was involved in transcriptional regulation. To confirm the hypothesis, we assessed the relationship between SNHG6 and PRC2. RIP results showed that SNHG6 could directly bind with EZH2 in BGC-823 and SGC-7901 cells but not bind with SUZ12 and EED (Fig. 5B), while U1 binding with SNRNP70 was used as positive control (Fig. 5C). Moreover, RNA-pulldown assay also confirmed that SNHG6 indeed binds with EZH2 in BGC-823 cells (Fig. 5D). And silenced EZH2 increased p27 expression both in mRNA and protein level (Fig. 5E). To determine whether SNHG6 is involved in transcriptional regulation through recruiting EZH2 to the target gene promoter, we applied ChIP assay. As revealed in Fig. 5F, the binding level of EZH2 and H3K27me3 in the promoter of p27 was significantly reduced when SNHG6 was knockdown. These results indicate that SNHG6 epigenetically modulate the expression of p27 through interacting with EZH2.

ZEB1 and p27 are involved in the oncogenic function of SNHG6 in GC cells

To verify the function of ZEB1 and p27 in GC, we measured the level of ZEB1 and p27 in GC tissues and corresponding normal tissues. As shown in Fig. 6A, the level of ZEB1 was obviously increased in GC tissues and was positively correlated with the level of SNHG6; whereas the level of p27 was significantly decreased in GC tissues and was negatively

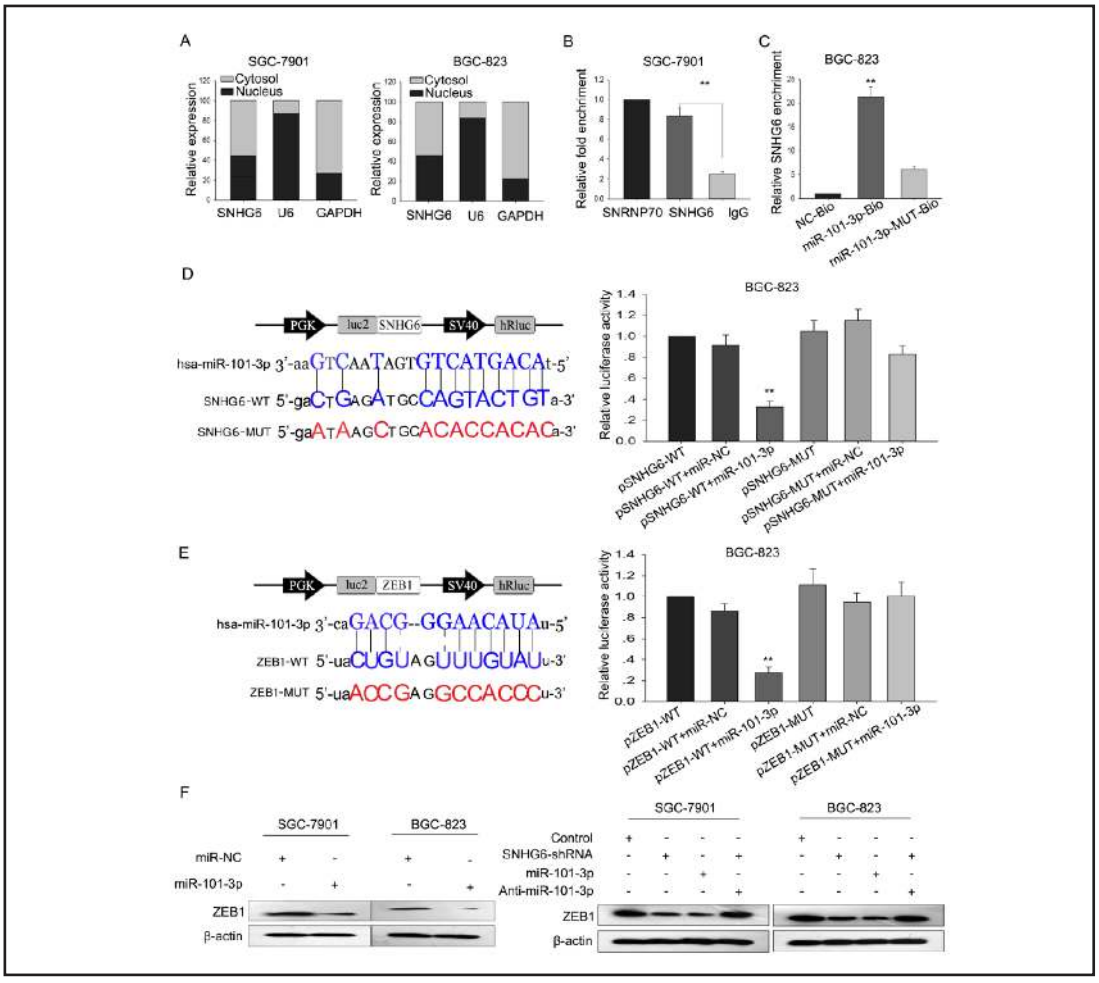

Fig. 4. SNHG6 exerted its pro-proliferation function through epigenetically silencing p27 transcription. A. Relative SNHG6 levels in SGC-7901 and BGC-823 cell cytoplasm or Nucleus were detected by qRT-PCR. GAPDH was used as cytoplasm control and U1 was used as nuclear control. B. Amount of SNHG6 levels in immunoprecipitates with Ago2 antibodies was measured by RT–qPCR. SNRNP70 RNA levels in immunoprecipitates with U1 antibodies were used as positive control. C. BGC-823 cells transfected with biotinylated WT miR-101-3p (miR-101-3p-Bio) or biotinylated mutant miR-101-3p (miR-101-3p-Mut-Bio) or biotinylated NC (NC-Bio), assayed by biotin-based pulldown 48 h after transfection. SNHG6 levels were analyzed by RT–qPCR. D. Wild-type (WT) SNHG6 cDNA containing putative miR-101-3p recognition sites or MUT sequence was cloned downstream of the luciferase gene in the pGL3-basic vector. The luciferase reporter plasmid containing WT or MUT was co-transfected into BGC-823 cells along miR-101-3p mimics in parallel with an empty plasmid vector. Luciferase activity was determined using a dual luciferase assay and shown as the relative luciferase activity normalized to Renilla activity. E. WT ZEB1 3'-UTR cDNA containing putative miR-101-3p recognition sites or the MUT sequence was cloned downstream of the luciferase gene in the pGL3-basic vector. Luciferase reporter plasmids containing WT or mutant ZEB1 3'-UTR were co-transfected into BGC-823 cells with miR-101-3p mimics in parallel with an empty plasmid vector. The data are presented as the relative luciferase activity normalized to Renilla activity. F. Western blot analysis showing the expression of ZEB1 in GC cells transfected with miR-101-3p mimics (left); western blot and quantitative RT-PCR analyses of ZEB1 expression after knockdown of SNHG6, overexpression of miR-101-3p or knockdown of SNHG6 + anti-miR-101-3p. *P<0.05, **P<0.01, Means±SD, was shown.

correlated with the level of SNHG6. Additionally, co-transfected ZEB1 and si-SNHG6 could abolish the anti-migration effect of si-SNHG6 of BGC-823 cells (Fig. 6B), and could reverse

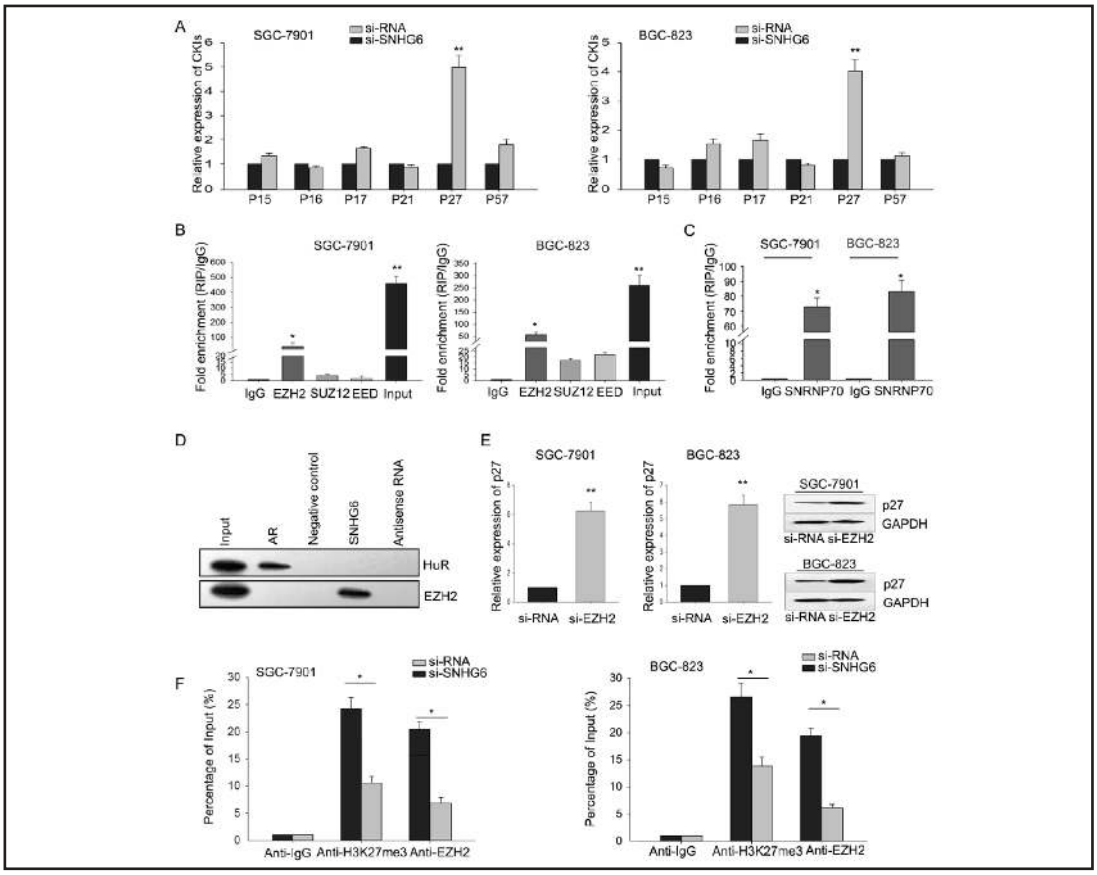

Fig. 5. SNHG6 exerted its pro-metastasis function through sponging miR-101-3p. A. qRT-PCR was used to detect mRNAs level of CKIs in SGC-7901 and BGC-823 cells with si-SNHG6. B. RIP experiments were performed using the EZH2, SUZ12, EED antibodies for immunoprecipitation. C. SNRNP70 RNA levels in immunoprecipitates with U1 antibodies were used as positive control. D. Biotinylated SNHG6 or antisense RNA was incubated with total-cell extracts (BGC-823 cells); EZH2 protein level in immunoprecipitates with SNHG6 RNA was determined by western blot assay. HuR protein immunoprecipitates with AR RNA was used as positive control. E. The level of p27 mRNA and protein level is measured by qRT-PCR and western blot assay when SNHG6 knockdown. F. ChIP-qRT-PCR of EZH2 occupancy and H3K27me3 binding in the p27 promoters in SGC-7901 and BGC-823 cells treated with si-SNHG6 or si-RNA; IgG as a negative control. *P<0.05, **P<0.01, Means±SD, was shown.

the MET to EMT (Fig. 6C-D). And silenced p27 could abrogate the anti-growth effect, G0/G1 arrest and apoptosis mediated by si-SNHG6 in BGC-823 cells (Fig. 6E-F). These findings revealed that ZEB1 and P27 are involved in the oncogenic function of SNHG6 in GC.

Discussion

In the past decades, the biological function of microRNAs (miRNAs) have been deeply studied in plenty types of cancer, including GC [22-27]. Currently, the newly uncovered lncRNAs, emerged as important factors in cellular processes and human diseases, have been attracting more and more attentions of researchers. For example, novel lncRNA TUSC7 was identified dysregulated in colorectal cancer and regulating cell proliferation through sponging miR-211 [28]. And lncRNA TRPM2-AS was demonstrated as novel prognostic marker and therapeutic target in prostate cancer [29]. In present study, we revealed that the expression level of SNHG6 in GC tissues was significantly increased compared with corresponding

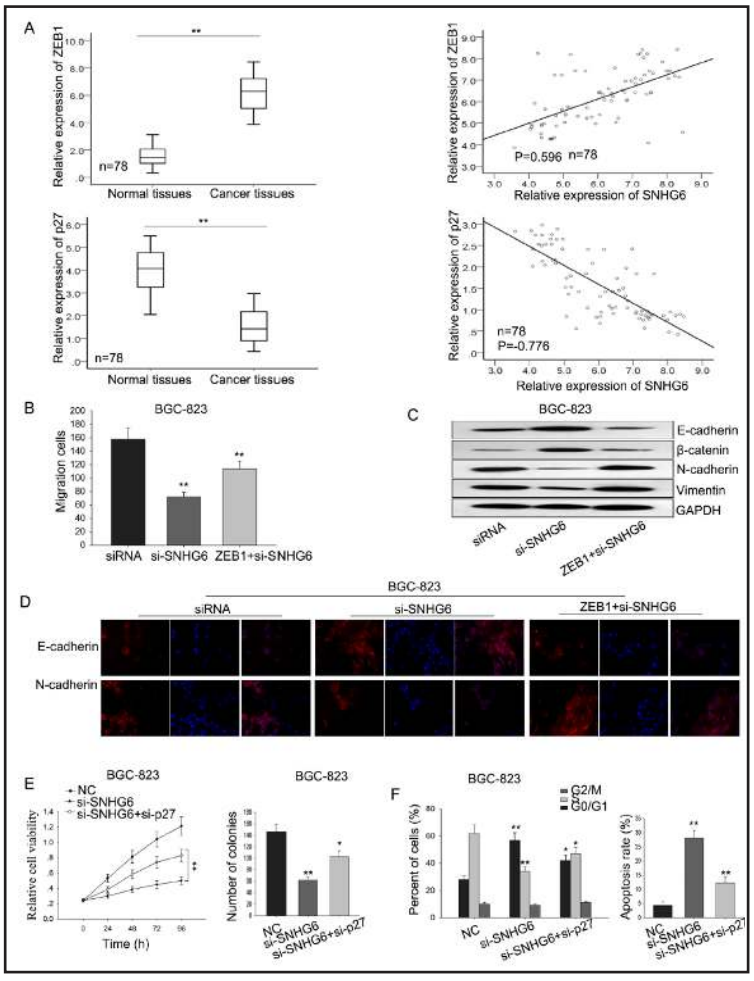

Fig. 6. ZEB1 and p27 are involved in the oncogenic function of SNHG6 in GC cells. A. The level of ZEB1 and p27 in GC tissues and corresponding normal tissues was measured by qRT-PCR (left); the correlation between SNHG6 and ZEB1 or p27 was analyzed by Spearman's correlation analysis. B. The weakened-migration capacity of BGC-823 cells caused by SNHG6 knockdown could be partially reversed by co-transfected with ZEB1. C-D. Western bolt and immunofluorescence assays were performed the EMT markers of BGC-823 cells transfected with siRNA, si-SNHG6 or ZEB1. E. MTT and colony formation assay was performed to determine the proliferation ability of BGC-823 cells transfected with siRNA, si-SNHG6 or ZEB1. F. Flow cytomeric analysis was performed to analyze the cell distribution and apoptosis rate BGC-823 cells transfected with siRNA, si-SNHG6 or ZEB1. *P<0.05, **P<0.01, Means±SD, was shown.

normal tissues. The high expression level of SNHG6 in GC patients was associated with invasion depth and TNM stage and positively correlated with poor prognosis and could be regarded as an independent prognostic indicator. Our findings indicated that SNHG6 acted as an oncogene and played a critical role in GC progression. It has been previously revealed that SNHG6 was upregulated in hepatocellular carcinoma (HCC) and regulated HCC progression. Despite the function of SNHG6 has been reported, the possible biological role and the underlying molecular mechanism of SNHG6 in GC has not been elucidated and still remains to be clarified. In our current study, the biological function of SNHG6 was explored by employing loss-of-function assay. We revealed that silenced SNHG6 could promote GC cell proliferation, migration and reverse EMT to MET. Mechanism experiments demonstrated that the growth-inhibition effect of si-SNHG6 was attributed to its influence on cell cycle and apoptosis, and si-SNHG6 mediated metastasis-inhibition and EMT to MET was dependent on its regulation on ZEB1.

In 2016, Chang et al. [21] demonstrated that SNHG6 plays an important role in the migration and EMT in HCCs through sponging miR-101-3p. In our study, mechanism experiments were performed and proved that si-SNHG6 mediated migration inhibition and EMT to MET was also through sponging miR-101-3p and thereby regulating the level of ZEB1. It has been studied that lncRNAs could interact with PRC2 and thereby epigenetically regulating the downstream targets [16, 17, 19, 30-33]. It is well known that activation of cyclinD-CDK4/6 kinases or inactivation of the CKIs could cause cell cycle disorders and influence cell proliferation [34]. CKIs, as tumor suppressors, are responsible for the modulation of the activity of Cdk/cyclin complexes [35]. And the aberrant methylation such as PRC2-mediated histone methylation in the CKI gene promoter region is associated with

gene expression suppression [36-39]. Additionally, plenty of lncRNAs have been reported to modulate specific genetic loci through recruiting PRC2 and PRC2-mediated epigenetic regulation play important role in tumorigenesis [17, 30, 31, 40-42]. In present study, our finding demonstrated that the deletion of SNHG6 could epigenetically silence the expression of p27 through interacting with EZH2.

Collectively, our study demonstrated a SNHG6-mediated regulation of the GC cell proliferation, cell cycle, cell apoptosis through epigenetically silencing p27 and metastasis through sponging miR-101-3p. Importantly, we first reported that SNHG6 serving as a member of PRC2-mediated epigenetic regulation participated in the development of GC. Our study might provide a strategy and contribute to the development of lncRNA-directed diagnostics and therapeutics against GC.

Acknowledgement

The authors thank the laboratory members.

Disclosure Statement

No conflicts of interest to disclose.

Reference

1 Coupland VH, Lagergren J, Luchtenborg M, Jack RH, Allum W, Holmberg L, Hanna GB, Pearce N, Moller H: Hospital volume, proportion resected and mortality from oesophageal and gastric cancer: a population-based study in England, 2004-2008. Gut 2013;62:961-966.

2 Ferlay J, Soerjomataram I, Dikshit R, Eser S, Mathers C, Rebelo M, Parkin DM, Forman D, Bray F: Cancer incidence and mortality worldwide: sources, methods and major patterns in GLOBOCAN 2012. Int J Cancer 2015;136:E359-386.

3 Camargo MC, Kim WH, Chiaravalli AM, Kim KM, Corvalan AH, Matsuo K, Yu J, Sung JJ, Herrera-Goepfert R, Meneses-Gonzalez F, Kijima Y, Natsugoe S, Liao LM, Lissowska J, Kim S, Hu N, Gonzalez CA, Yatabe Y, Koriyama C, Hewitt SM, Akiba S, Gulley ML, Taylor PR, Rabkin CS: Improved survival of gastric cancer with tumour Epstein-Barr virus positivity: an international pooled analysis. Gut 2014;63:236-243.

4 Duraes C, Almeida GM, Seruca R, Oliveira C, Carneiro F: Biomarkers for gastric cancer: prognostic, predictive or targets of therapy? Virchows Arch 2014;464:367-378.

5 Zhou Q, Zheng X, Chen L, Xu B, Yang X, Jiang J, Wu C: Smad2/3/4 Pathway Contributes to TGF-beta-Induced MiRNA-181b Expression to Promote Gastric Cancer Metastasis by Targeting Timp3. Cell Physiol Biochem 2016;39:453-466.

6 Wang X, Li T, Li M, Cao N, Han J: The Functional SOCS3 RS115785973 Variant Regulated by MiR-4308 Promotes Gastric Cancer Development in Chinese Population. Cell Physiol Biochem 2016;38:1796-1802.

7 Zhu P, Zhang J, Zhu J, Shi J, Zhu Q, Gao Y: MiR-429 Induces Gastric Carcinoma Cell Apoptosis Through Bcl-2. Cell Physiol Biochem 2015;37:1572-1580.

8 Wang D, Fan Z, Liu F, Zuo J: Hsa-miR-21 and Hsa-miR-29 in Tissue as Potential Diagnostic and Prognostic Biomarkers for Gastric Cancer. Cell Physiol Biochem 2015;37:1454-1462.

9 Liu Y, Xu J, Jiang M, Ni L, Chen Y, Ling Y: Association between functional PSMD10 Rs111638916 variant regulated by MiR-505 and gastric cancer risk in a Chinese population. Cell Physiol Biochem 2015;37:1010-1017.

10 Chen Q, Qin R, Fang Y, Li H, Liu Y: A Functional Variant at the miR-214 Binding Site in the Methylenetetrahydrofolatereductase Gene Alters Susceptibility to Gastric Cancer in a Chinese Han Population. Cell Physiol Biochem 2015;36:622-630.

11 Zhang CL, Zhu KP, Ma XL: Antisense lncRNA FOXC2-AS1 promotes doxorubicin resistance in osteosarcoma by increasing the expression of FOXC2. Cancer Lett 2017;396:66-75.

12 Qian Y, Liu D, Cao S, Tao Y, Wei D, Li W, Li G, Pan X, Lei D: Upregulation of the long noncoding RNA UCA1 affects the proliferation, invasion, and survival of hypopharyngeal carcinoma. Mol Cancer 2017;16:68.
13 Correction: Long Noncoding RNA GCASPC, a Target of miR-17-3p, Negatively Regulates Pyruvate Carboxylase-Dependent Cell Proliferation in Gallbladder Cancer. Cancer Res 2017;77:1503.
14 Lv J, Fan HX, Zhao XP, Lv P, Fan JY, Zhang Y, Liu M, Tang H: Long non-coding RNA Unigene56159 promotes epithelial-mesenchymal transition by acting as a ceRNA of miR-140-5p in hepatocellular carcinoma cells. Cancer Lett 2016;382:166-175.
15 Zhou X, Ye F, Yin C, Zhuang Y, Yue G, Zhang G: The Interaction Between MiR-141 and lncRNA-H19 in Regulating Cell Proliferation and Migration in Gastric Cancer. Cell Physiol Biochem 2015;36:1440-1452.
16 Lin PC, Huang HD, Chang CC, Chang YS, Yen JC, Lee CC, Chang WH, Liu TC, Chang JG: Long noncoding RNA TUG1 is downregulated in non-small cell lung cancer and can regulate CELF1 on binding to PRC2. BMC Cancer 2016;16:583.
17 Sun M, Nie F, Wang Y, Zhang Z, Hou J, He D, Xie M, Xu L, De W, Wang Z, Wang J: LncRNA HOXA11-AS Promotes Proliferation and Invasion of Gastric Cancer by Scaffolding the Chromatin Modification Factors PRC2, LSD1, and DNMT1. Cancer Res 2016;76:6299-6310.
18 Li L, Dang Q, Xie H, Yang Z, He D, Liang L, Song W, Yeh S, Chang C: Correction: Infiltrating mast cells enhance prostate cancer invasion via altering LncRNA-HOTAIR/PRC2-androgen receptor (AR)-MMP9 signals and increased stem/progenitor cell population. Oncotarget 2016;7:83828.
19 Liu Z, Sun M, Lu K, Liu J, Zhang M, Wu W, De W, Wang Z, Wang R: The long noncoding RNA HOTAIR contributes to cisplatin resistance of human lung adenocarcinoma cells via downregualtion of p21(WAF1/CIP1) expression. PLoS One 2013;8:e77293.
20 Cao C, Zhang T, Zhang D, Xie L, Zou X, Lei L, Wu D, Liu L: The long non-coding RNA, SNHG6-003, functions as a competing endogenous RNA to promote the progression of hepatocellular carcinoma. Oncogene 2017;36:1112-1122.
21 Chang L, Yuan Y, Li C, Guo T, Qi H, Xiao Y, Dong X, Liu Z, Liu Q: Upregulation of SNHG6 regulates ZEB1 expression by competitively binding miR-101-3p and interacting with UPF1 in hepatocellular carcinoma. Cancer Lett 2016;383:183-194.
22 Li S, Zhang H, Ning T, Wang X, Liu R, Yang H, Han Y, Deng T, Zhou L, Zhang L, Bai M, Wang X, Ge S, Ying G, Ba Y: MiR-520b/e Regulates Proliferation and Migration by Simultaneously Targeting EGFR in Gastric Cancer. Cell Physiol Biochem 2016;40:1303-1315.
23 Wang B, Yang H, Shen L, Wang J, Pu W, Chen Z, Shen X, Fu J, Zhuang Z: Rs56288038 (C/G) in 3'UTR of IRF-1 Regulated by MiR-502-5p Promotes Gastric Cancer Development. Cell Physiol Biochem 2016;40:391-399.
24 Hou CG, Luo XY, Li G: Diagnostic and Prognostic Value of Serum MicroRNA-206 in Patients with Gastric Cancer. Cell Physiol Biochem 2016;39:1512-1520.
25 Xiang XJ, Deng J, Liu YW, Wan LY, Feng M, Chen J, Xiong JP: MiR-1271 Inhibits Cell Proliferation, Invasion and EMT in Gastric Cancer by Targeting FOXQ1. Cell Physiol Biochem 2015;36:1382-1394.
26 Li X, Li H, Zhang R, Liu J, Liu J: MicroRNA-449a inhibits proliferation and induces apoptosis by directly repressing E2F3 in gastric cancer. Cell Physiol Biochem 2015;35:2033-2042.
27 Wang QX, Zhu YQ, Zhang H, Xiao J: Altered MiRNA expression in gastric cancer: a systematic review and meta-analysis. Cell Physiol Biochem 2015;35:933-944.
28 Xu J, Zhang R, Zhao J: The Novel Long Noncoding RNA TUSC7 Inhibits Proliferation by Sponging MiR-211 in Colorectal Cancer. Cell Physiol Biochem 2017;41:635-644.
29 Orfanelli U, Jachetti E, Chiacchiera F, Grioni M, Brambilla P, Briganti A, Freschi M, Martinelli-Boneschi F, Doglioni C, Montorsi F, Bellone M, Casari G, Pasini D, Lavorgna G: Antisense transcription at the TRPM2 locus as a novel prognostic marker and therapeutic target in prostate cancer. Oncogene 2015;34:2094-2102.
30 Portoso M, Ragazzini R, Brencic Z, Moiani A, Michaud A, Vassilev I, Wassef M, Servant N, Sargueil B, Margueron R: PRC2 is dispensable for HOTAIR-mediated transcriptional repression. 2017;10.15252/embj.201695335
31 Sun CC, Li SJ, Li G, Hua RX, Zhou XH, Li DJ: Long Intergenic Noncoding RNA 00511 Acts as an Oncogene in Non-small-cell Lung Cancer by Binding to EZH2 and Suppressing p57. Mol Ther Nucleic Acids 2016;5:e385.
32 Conway E, Healy E, Bracken AP: PRC2 mediated H3K27 methylations in cellular identity and cancer. Curr Opin Cell Biol 2015;37:42-48.

33 Zhang EB, Yin DD, Sun M, Kong R, Liu XH, You LH, Han L, Xia R, Wang KM, Yang JS, De W, Shu YQ, Wang ZX: P53-regulated long non-coding RNA TUG1 affects cell proliferation in human non-small cell lung cancer, partly through epigenetically regulating HOXB7 expression. Cell Death Dis 2014;5:e1243.
34 Sherr CJ, McCormick F: The RB and p53 pathways in cancer. Cancer Cell 2002;2:103-112.
35 Lim S, Kaldis P: Cdks, cyclins and CKIs: roles beyond cell cycle regulation. Development 2013;140:3079-3093.
36 Daa T, Kashima K, Kondo Y, Yada N, Suzuki M, Yokoyama S: Aberrant methylation in promoter regions of cyclin-dependent kinase inhibitor genes in adenoid cystic carcinoma of the salivary gland. Apmis 2008;116:21-26.
37 Paul TA, Bies J, Small D, Wolff L: Signatures of polycomb repression and reduced H3K4 trimethylation are associated with p15INK4b DNA methylation in AML. Blood 2010;115:3098-3108.
38 Aoki R, Chiba T, Miyagi S, Negishi M, Konuma T, Taniguchi H, Ogawa M, Yokosuka O, Iwama A: The polycomb group gene product Ezh2 regulates proliferation and differentiation of murine hepatic stem/progenitor cells. J Hepatol 2010;52:854-863.
39 Yang X, Karuturi RK, Sun F, Aau M, Yu K, Shao R, Miller LD, Tan PB, Yu Q: CDKN1C (p57) is a direct target of EZH2 and suppressed by multiple epigenetic mechanisms in breast cancer cells. PLoS One 2009;4:e5011.
40 Woo CJ, Maier VK, Davey R, Brennan J, Li G, Brothers J, 2nd, Schwartz B, Gordo S, Kasper A, Okamoto TR, Johansson HE, Mandefro B, Sareen D, Bialek P, Chau BN, Bhat B, Bullough D, Barsoum J: Gene activation of SMN by selective disruption of lncRNA-mediated recruitment of PRC2 for the treatment of spinal muscular atrophy. Proc Natl Acad Sci U S A 2017;114:E1509-e1518.
41 Terashima M, Tange S, Ishimura A, Suzuki T: MEG3 Long Noncoding RNA Contributes to the Epigenetic Regulation of Epithelial-Mesenchymal Transition in Lung Cancer Cell Lines. J Biol Chem 2017;292:82-99.
42 Sun CC, Li SJ, Li G, Hua RX, Zhou XH, Li DJ: Long Intergenic Noncoding RNA 00511 Acts as an Oncogene in Non-small-cell Lung Cancer by Binding to EZH2 and Suppressing p57. Embo j 2016;5:e385.